

Conf-921082--2

Estimating The Water Table Under The Radioactive Waste Management Site in Area 5 of the Nevada Test Site
The Dupuit - Forcheimer Approximation

CONF-921082--2

DE92 013506

by
F. Tom Lindstrom, Lawrence E. Barker, David E. Cawfield,
Dale D. Daffern, Brian L. Dozier, Dudley F. Emer, Warren R. Strong

Reynolds Electrical & Engineering Co., Inc.
Post Office Box 98521
Las Vegas, NV 89193-8521

RECEIVED
11 1992

ABSTRACT

To adequately manage the low level nuclear waste (LLW) repository in Area 5 of the Nevada Test Site (NTS), a knowledge of the water table under the site is paramount. The estimated thickness of the arid intermountain basin alluvium is roughly 900 feet. Very little reliable water table data for Area 5 currently exists. The Special Projects Section of the Reynolds Electrical & Engineering Co., Inc. Waste Management Department is currently formulating a long-range drilling and sampling plan in support of a Resource Conservation Recovery Act (RCRA) Part B permit waiver for groundwater monitoring and liner systems. An estimate of the water table under the LLW repository, called the Radioactive Waste Management Site (RWMS) in Area 5, is needed for the drilling and sampling plan. Very old water table elevation estimates at about a dozen widely scattered test drill holes, as well as water wells, are available from declassified U.S. Geological Survey, Lawrence Livermore National Laboratory, and Los Alamos National Laboratory drilling logs. A three-dimensional steady-state water-flow equation for estimating the water table elevation under a thick, very dry vadose zone is developed using the Dupuit assumption. A prescribed positive vertical downward infiltration/evaporation condition is assumed at the atmosphere/soil interface. An approximation to the square of the elevation head, based upon multivariate cubic interpolation methods, is introduced. The approximate is forced to satisfy the governing elliptic (Poisson) partial differential equation over the domain of definition. The remaining coefficients are determined by interpolating the water table at eight "boundary points." Several realistic scenarios approximating the water table under the RWMS in Area 5 of the NTS are discussed.

ACKNOWLEDGEMENT

The authors wish to thank Dr. Lynn Ebeling of Reynolds Electrical & Engineering Co., Inc. (REECo) and Dr. Britt Jacobson of the Reno, Nevada branch of the Desert Research Institute for their helpful reviews of this manuscript. We also wish to thank Patricia Herrin and Yvonne Lewis of the REECo Information Products Section for their invaluable help in typing, proofreading, and assembling this manuscript.

1
DISTRIBUTION OF THIS DOCUMENT IS UNLIMITED

MASTER

1.0 INTRODUCTION

The Dupuit (1863) approximation has been used by groundwater modelers and hydrologists in a variety of situations (Hantush, 1967; Bear and Verruijt, 1987). It works well when the slope of the water table in a phreatic aquifer is very small. Slopes varying from a one-foot (ft) rise in a 1,000-foot run to a ten-foot rise in 1,000-foot run are quite common. Besides the assumption of shallow slope over the domain of definition (i.e., that portion in the x-y plane over which the hydraulic head H is defined) D , the assumption of a thin capillary fringe relative to the thickness of the entire vadose zone is made. For example, a capillary fringe six feet thick relative to a total vadose zone thickness of 900 feet, qualifies. Also, with the assumption of shallow slopes along the water table, the assumption of horizontal equipotentials is made. Bear and Verruijt (1987) give a good introductory discussion of the Dupuit or Dupuit-Forcheimer (D-F) concepts on pages 45-52 of their book.

The phreatic surface or water table elevation head H , neglecting the capillary fringe pressure (suction or tension), is assumed to be a surface of constant atmospheric pressure. Using the above mentioned concepts, Lindstrom et al. (1992) derived a two-dimensional Dupuit-Forcheimer approximation to the water table under the Radioactive Waste Management Site (RWMS) in Area 5 at the Nevada Test Site (NTS). Figure 1 shows the location of NTS in Nevada.

2.0 GOVERNING EQUATION

2.1 Assumptions

It is assumed that:

1. The slope of the phreatic surface is much smaller than 0.1 ft/ft.
2. The bottom of the aquifer is flat and impermeable.
3. The recharge (infiltration)-exfiltration (evaporation) rate q_{rchg} (ft/day) can be represented by a bilinear expression.
4. The aquifer is homogenous and isotropic with respect to hydraulic conductivity K (ft/day).

The governing equation can be written as

$$\frac{\partial^2 H^2}{\partial x^2} + \frac{\partial^2 H^2}{\partial y^2} = -2 q_{rchg}/K \quad , \quad (1)$$

which is a Poisson (elliptic) partial differential equation (pde) in the square of the water table elevation head H (ft) relative to mean sea level as the reference datum.

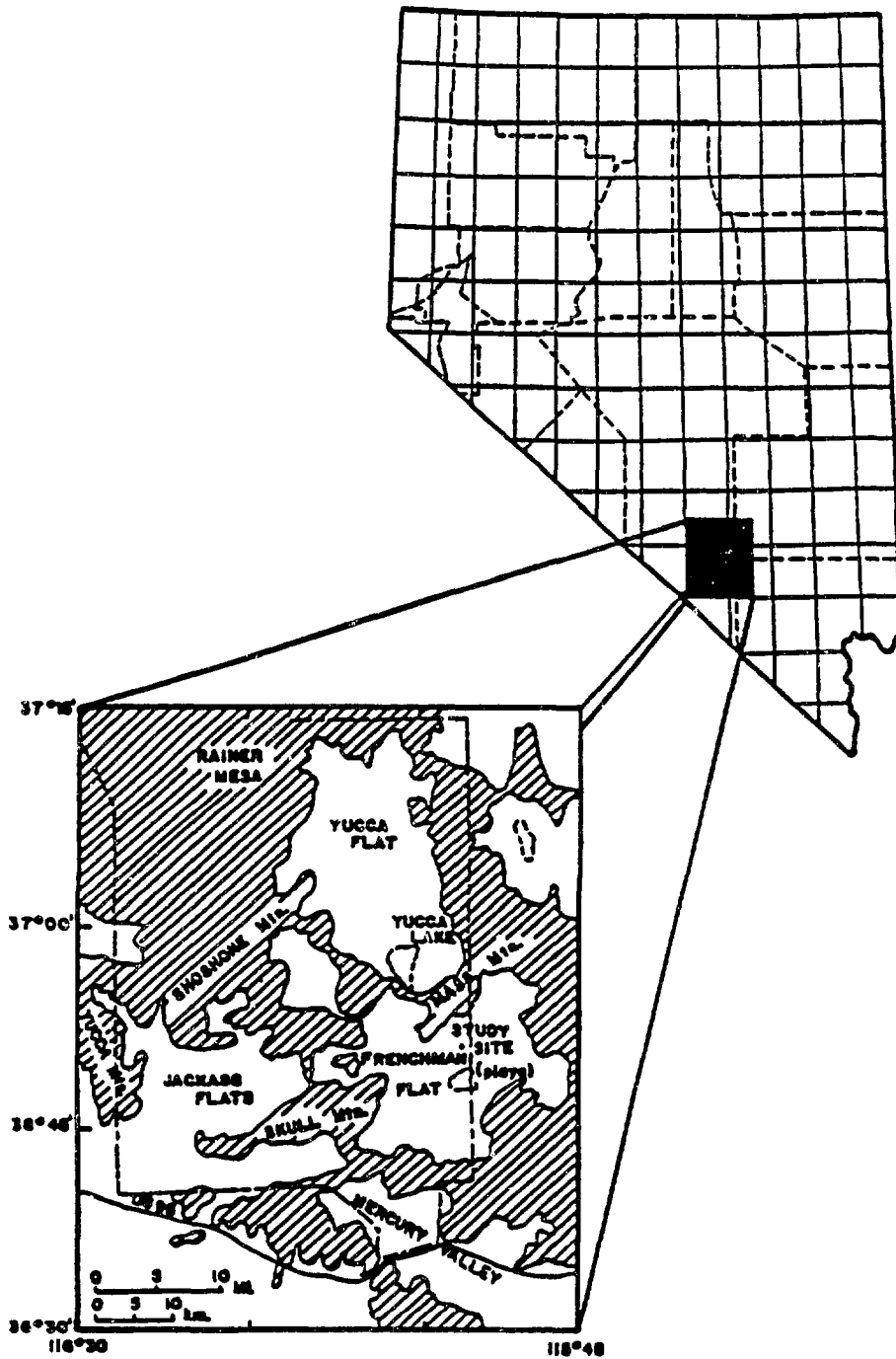


Figure 1. Map of Nevada showing the location of the Nevada Test Site.

The domain of definition \mathfrak{D} together with its boundary Γ is sketched in Figure 2. The point (x_0, y_0) in \mathfrak{D} is called the expansion point for the approximate solution. The four outer heavy dots represent the locations of the four calibration points for representing the infiltration/evaporation function q_{rchg} as a bilinear form.

Since we know neither $H(x,y)$ nor the normal derivative ($\frac{\partial H}{\partial x}$ and $\frac{\partial H}{\partial y}$ components) at every point along Γ , we cannot solve Equation 1 in the classical boundary value sense via eigenfunction expansion methods. We introduce an approximate solution to $H(x,y)$ that will require knowing H at eight calibration points together with representing q_{rchg} as a bilinear form. The eight calibration well locations are also shown in Figure 2.

3.0 APPROXIMATE SOLUTION

Lindstrom et al. (1992) give the details of the approximate solution method. A brief summary of their work follows.

The superposition principle allows writing

$$H^2(x,y) = H_L^2(x,y) + H_p^2(x,y) \quad , \quad (2)$$

where H_L^2 satisfies the Laplace problem

$$\frac{\partial^2 H_L^2}{\partial x^2} + \frac{\partial^2 H_L^2}{\partial y^2} = 0, \text{ for all } (x,y) \text{ in } \mathfrak{D} \quad (3)$$

and

$$H_L^2 = \sum_{i=0}^7 A_i \Phi_i(x,y) \quad . \quad (4)$$

Span $\{\Phi_0, \Phi_1, \dots, \Phi_7\}$ forms a basis for a real linear vector sub space of dimension eight of the real linear vector space (dimension 16) of all multivariate polynomials in two variables of degree three or less. The eight Φ 's are defined in Appendix B. The eight A_i 's are found as the elements of the solution vector of the linear system

$$X A = H_L^2 \quad , \quad (5)$$

DISCLAIMER

This report was prepared as an account of work sponsored by an agency of the United States Government. Neither the United States Government nor any agency thereof, nor any of their employees, makes any warranty, express or implied, or assumes any legal liability or responsibility for the accuracy, completeness, or usefulness of any information, apparatus, product, or process disclosed, or represents that its use would not infringe privately owned rights. Reference herein to any specific commercial product, process, or service by trade name, trademark, manufacturer, or otherwise does not necessarily constitute or imply its endorsement, recommendation, or favoring by the United States Government or any agency thereof. The views and opinions of authors expressed herein do not necessarily state or reflect those of the United States Government or any agency thereof.

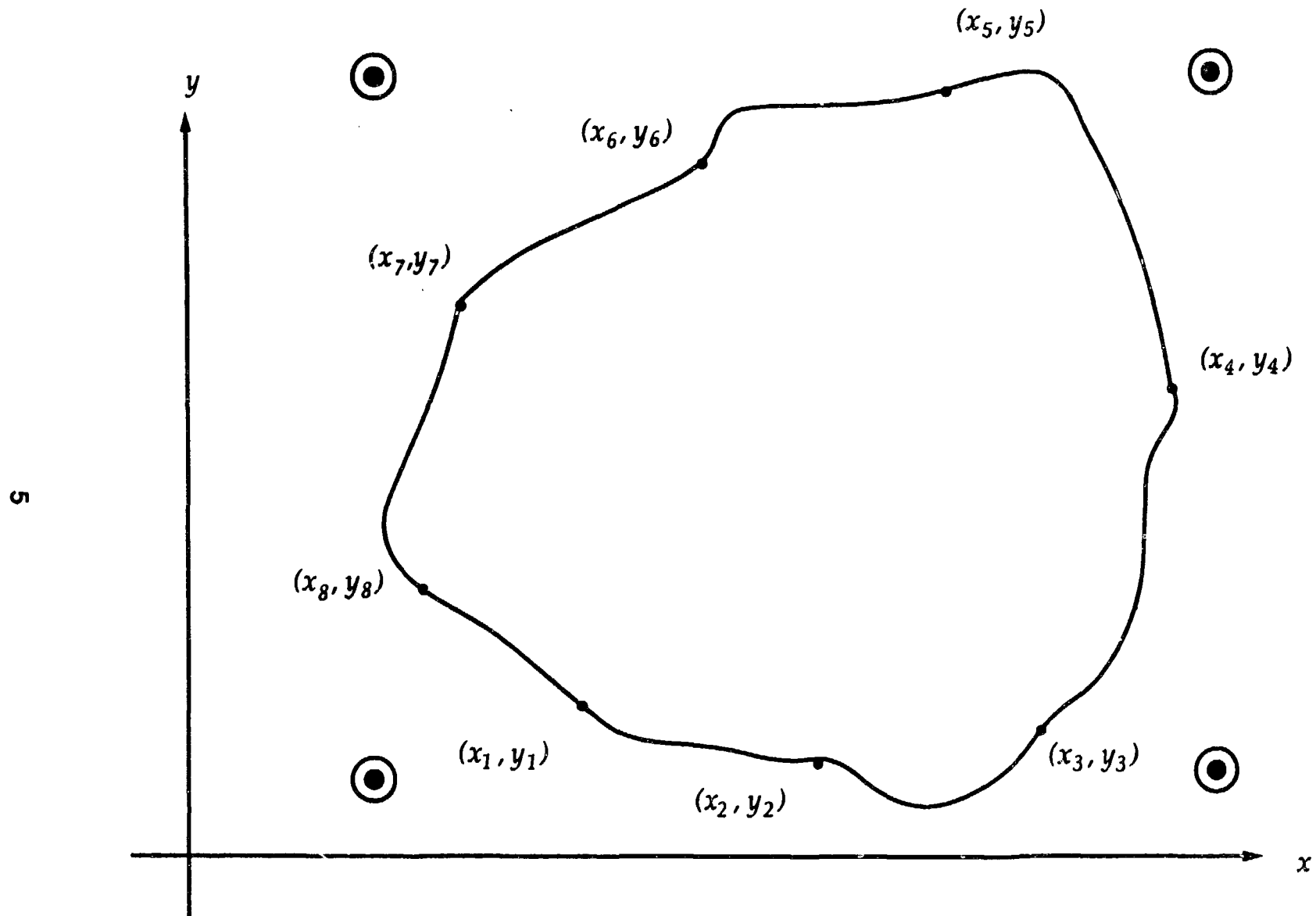


Figure 2. Sketch of domain D with boundary Γ .

where the 8x8 dense "design matrix" X has the structure

$$X = \begin{bmatrix} \Phi_0(x_1, y_1) & \Phi_1(x_1, y_1) & \Phi_2(x_1, y_1) & \cdot & \cdot & \cdot & \Phi_7(x_1, y_1) \\ \Phi_0(x_8, y_8) & \Phi_1(x_8, y_8) & \cdot & \cdot & \cdot & \cdot & \Phi_7(x_8, y_8) \end{bmatrix}, \quad (6)$$

the "known" vector H_L^2 has the structure

$$H_L^2 = (H^2(x_1, y_1), H^2(x_2, y_2), \dots, H^2(x_8, y_8))^T, \quad (7)$$

and the "unknown" vector A of coefficients has the structure

$$A = (A_0, A_1, A_2, \dots, A_7)^T. \quad (8)$$

H_p^2 satisfies the Poisson problem

$$\frac{\partial^2 H_p^2}{\partial x^2} + \frac{\partial^2 H_p^2}{\partial y^2} = \frac{-2 q_{rchg}(x, y)}{K} \quad (9)$$

with

$$q_{rchg}(x, y) = \beta_0 + \beta_1(x - x_0) + \beta_2(y - y_0) + \beta_3(x - x_0)(y - y_0), \quad (10)$$

(Box, Hunter, and Hunter, 1978; Prenter, 1975) and

$$H_p^2 = \sum_{i=0}^7 B_i \Phi_i(x, y) + \gamma(x, y), \quad (11)$$

where

$$\gamma(x, y) = \frac{-(y - y_0)^2}{K} \left(\beta_0 + \beta_1(x - x_0) + \frac{\beta_2}{3}(y - y_0) + \frac{\beta_3}{3}(x - x_0)(y - y_0) \right). \quad (12)$$

Since the eight calibration well elevations have already been used in estimating \underline{A} , we follow the classical pde approach and set $H_p^2 = 0$ at each of the eight calibration well locations. We then have the linear system

$$\underline{XB} = -\underline{\gamma} \quad , \quad (13)$$

where X is defined in Equation 6 and $\underline{\gamma}$ is defined as

$$\underline{\gamma} = (\gamma(x_1, y_1), \gamma(x_2, y_2), \gamma(x_3, y_3), \dots, \gamma(x_8, y_8))^T \quad . \quad (14)$$

With all the A_i and B_i coefficients thusly known, Equation 2 is used to find $H^2(x, y)$ for any (x, y) in \mathcal{D} . Actually, the positive square root is chosen, since it is conventional to discuss H rather than H^2 .

A word of warning is in order. X can be singular for certain well patterns (geometries). The choice of well patterns is thus an important issue. We are currently researching the "optimal design" well pattern problem based on the above outlined D-F model. The D'Arcy specific discharge components q_x and q_y are calculated at each point (x, y) in \mathcal{D} by using the formulas

$$q_x = -K \frac{\partial H}{\partial x} = -\frac{K}{2} \frac{\frac{\partial H_L^2}{\partial x} + \frac{\partial H_p^2}{\partial x}}{H} \quad (\text{ft/day}) \quad (15)$$

and

$$q_y = -K \frac{\partial H}{\partial y} = -\frac{K}{2} \frac{\frac{\partial H_L^2}{\partial y} + \frac{\partial H_p^2}{\partial y}}{H} \quad . \quad (\text{ft/day}) \quad (16)$$

4.0 APPLICATION OF THE D-F MODEL

A summary of the currently believed basin-wide geology and hydrology of the 15-mile diameter closed basin called Frenchman Flat is given in Lindstrom et al. (1992). They also give a summary of the precipitation pattern as documented in Winograd and Thordarson (1975). Suffice it to say that the region is very arid (<5 inches total precipitation per year). The vadose zone is about 240 meters (780 ft) thick and is comprised of gravelly, sandy alluvium. The alluvium is largely derived from tuffaceous rock in the surrounding mountains.

4.1 Original Calibration Drill Holes/Water Wells

The primary mission of the NTS over the past 40 years has been the testing of nuclear weapons. Since the end of above ground testing in 1962, nuclear devices have been detonated well below the ground surface. This has required the drilling of large diameter, deep boreholes. Unfortunately, though there have been five (Neagle, 1992) underground nuclear devices detonated at or near the north end of Frenchman Flat (and about ten other mixed water well and test boreholes scattered throughout Frenchman Flat), very scanty geology and hydrology data exist for all these drill holes.

Accurate measurements of the water table depth are absent from most records. Some water wells, as well as post-test drillback holes, exist in Frenchman Flat. Figure 3 shows a sketch of the location of several of the drill holes/water wells closest to the RWMS. Water table elevations are also shown, but these are more than likely estimated. A crescent-shaped region can be envisioned for \mathcal{D} (Figure 3). The design matrix X was found to be nonsingular and mildly ill-conditioned using the geometric locations of the eight calibration drill holes/wells given in Table 1. Our own linear system solver using Gauss elimination with full pivoting and iterative improvement (Young and Gregory, 1973), was used to find the \underline{A} and \underline{B} vectors of coefficients. Using these coefficients and assuming $q_{rchg} \equiv 0$ over \mathcal{D} , the estimated water table under RWMS is shown as a contour plot in Figure 4. Figure 4 clearly shows the water at the water table to be flowing in an east-southeasterly direction with specific discharge components $q_x = 0.075$ ft/day and $q_y = -0.026$ ft/day, based on a K value of 30.0 ft/day (Daifern et al., 1990). This places the water flow towards the center of the playa in Frenchman Flat.

4.2 Monte Carlo Estimated Water Table Under the RWMS

The eight calibration drill hole/water well elevations used in generating the estimated water table under RWMS (simulation 2, above) were gathered from various U.S. Geological Survey and Lawrence Livermore National Laboratory maps and drilling logs over about a 20-year time span. Since the primary concern of the drillers was generally not in logging the depth to the water table, some of the water table elevations may be in considerable error. Also, the region of calibration is an area roughly 25,000 feet in diameter. It is highly unlikely that there are no intervening geologic structures in the water table region. The D-F model used here assumes that the water table region has homogeneous and areally isotropic, hydrologic properties. This is a very big assumption and one which is probably not true on such a grand scale as 25,000 feet. Therefore, the following uncertainty analysis is in order.

A rather exhaustive literature and personal telephone interview survey yields the currently believed water table elevations in the original eight drill holes/water wells used for calibration. Table 2 summarizes this data. Figure 5 shows the estimated water table under RWMS based upon these latest findings.

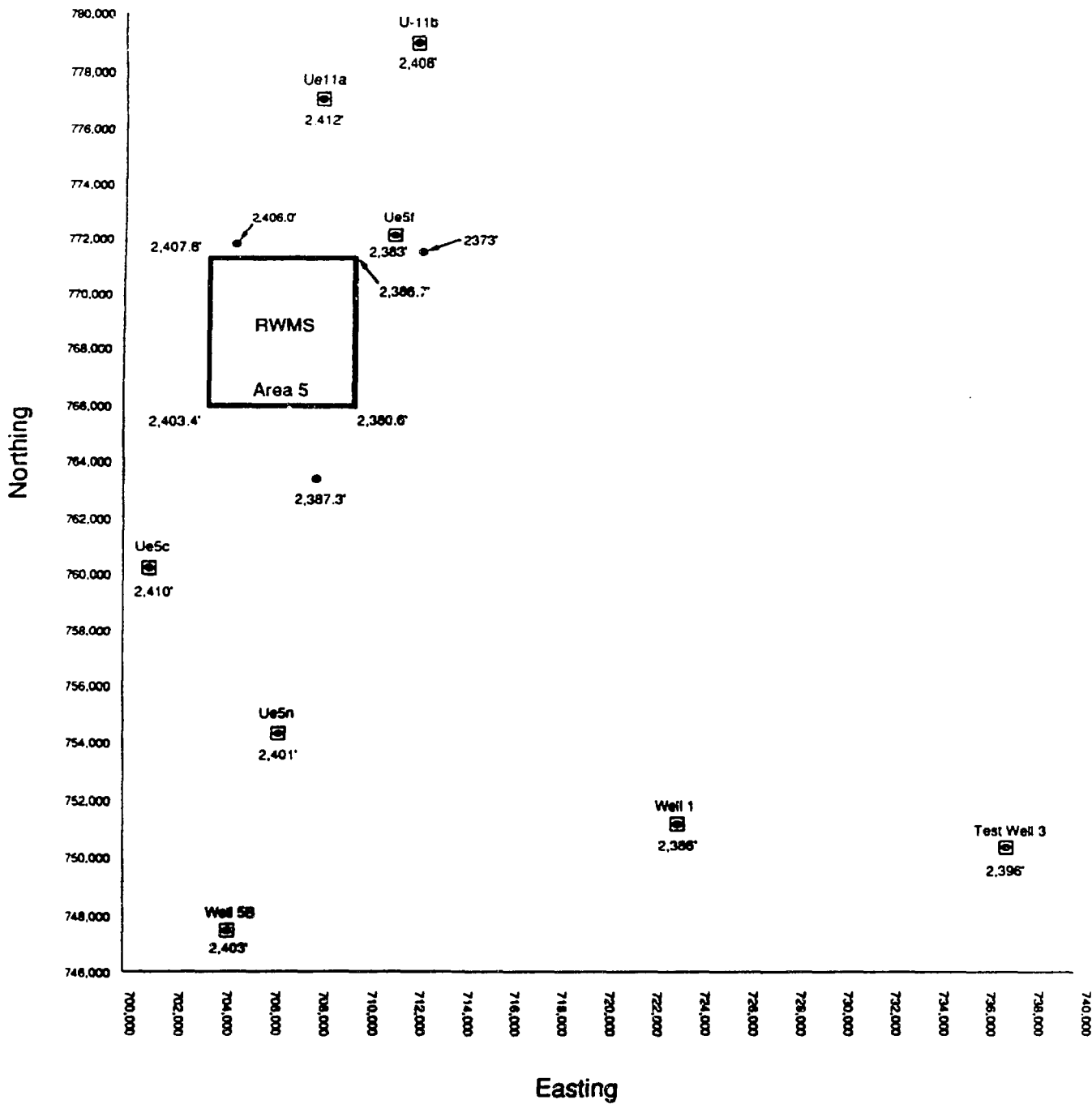


Figure 3. Location of eight calibration drill holes/water wells used in the D-F model.

Table 1. Nevada Coordinates* and Water Table Elevations of the Eight Calibration Drill Holes/Water Wells.

Calibration Point	Easting x (ft)	Northing y (ft)	Elevation Above Mean Sea Level** H (ft)	Name
1	706,414.0	754,460.0	2,401.0	UE5N
2	701,000.0	760,130.0	2,410.0	UE5C
3	736,937.0	750,189.0	2,396.0	TEST WELL 3
4	708,280.0	777,130.0	2,412.0	UE11A
5	710,901.0	772,498.0	2,383.0	UE5F
6	712,275.0	778,800.0	2,408.0	U11B
7	704,263.0	747,359.0	2,410.0	WELL 5b
8	723,349.0	751,509.0	2,386.0	WELL 1

*Nevada Coordinate System is an arbitrarily chosen rectangular right Cartesian coordinate system historically set up in the late 1800's by the land surveyors.

**Water table elevation estimates were obtained from various U.S. Geological Survey (USGS), Lawrence Livermore National Laboratory, and Los Alamos National Laboratory drilling logs supplied by the USGS reference library in Mercury, NV.

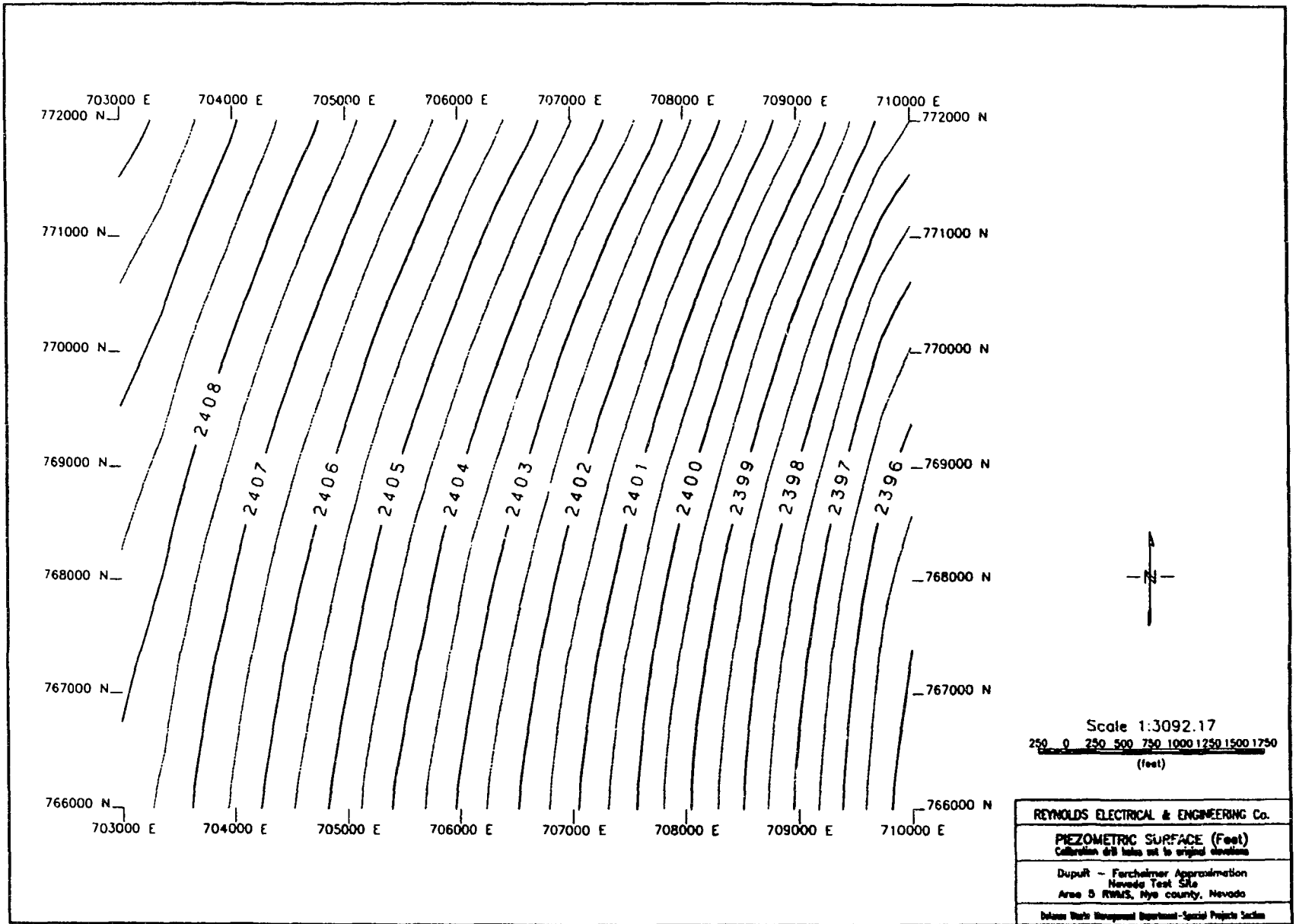


Figure 4. All calibration drill holes/water wells, set to original elevations given in Table 1. The four corners of the coordinates coincide with the four corners of the RWMS.

Table 2. Nevada Coordinates* and "Best Estimates" of Water Table Elevations of the Eight Calibration Drill Holes/Water Wells

Calibration Point	Easting x (ft)	Northing y (ft)	Elevation Above Mean Sea Level H (ft)	Name
1	704,809.0	755,119.0	2,410, ± 2 ft	RNM2S
2	701,000.0	760,130.0	2,410, ± 2 ft	UE5C
3	736,937.0	750,189.0	2,395, ± 1 ft	TEST WELL 3
4	708,280.0	777,130.0	2,410, ± 2 ft	UE11A
5	710,901.0	772,498.0	2,410, ± 2 ft	UE5F
6	712,275.0	778,800.0	2,410, ± 2 ft	U11B
7	704,263.0	747,259.0	2,410, -i to +3 ft	WELL 5b
8	723,349.0	751,509.0	2,386, ± 15 ft	WELL 1

*Nevada Coordinate System is an arbitrarily chosen rectangular right Cartesian coordinate system historically set up in the late 1800's by the land surveyors.

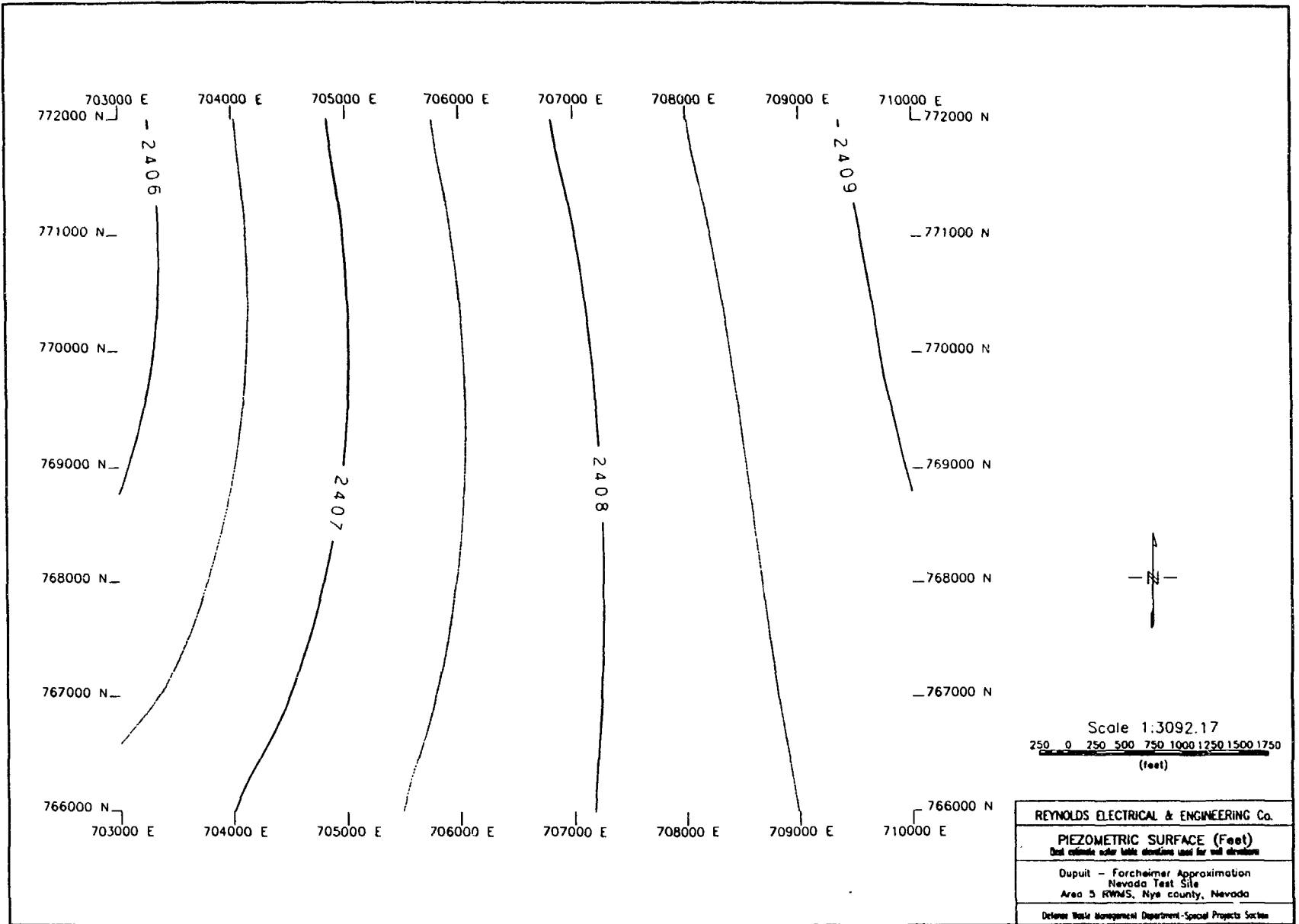


Figure 5. Best estimates of water table elevations used for calibration dill hole/water well elevations.

In comparing Tables 1 and 2, we observe a mean elevation increase of 27 feet in drill hole UE5F, which is a major elevation change. The other changes are less than or equal to two feet. Observe the major uncertainty value associated with Well 1. Very poor drilling logs exist for this water well, hence, the major uncertainty in its mean elevation.

In comparing Tables 1 and 2, we observe the substitution of drill hole RNM2S for UE5N. The measured water table elevation at UE5N differed dramatically from those of nearby wells and drill holes. This suggests that the measurement might be substantially in error or affected by notably different geology. Additionally, the water table elevation at drill hole UE5F increased by 27 feet, which is a major change. No other difference exceeded two feet.

A Monte Carlo analysis was used to assess the impact of water table elevation uncertainties. Probability distributions, detailed below, were placed on each water table elevation. Using the random number generator from the statistics package MINITAB release 7.1, 3,000 realizations of the simulated elevations were run. For each realization, water table elevations within RWMS were estimated using the approximation described here with constant recharge of 0.0 ft/day.

Random water table elevations were assumed statistically independent. All elevations except Well 5b were assumed normally distributed, with the mean equal to the observed water table elevation and standard deviation of one-half the stated error. Well 1 was drilled for reasons other than water table characterization, and hence has a large associated uncertainty. Due to asymmetric uncertainty, the water table elevation at Well 5b was assumed to be lognormally distributed. The 2.5th and 97.5th percentiles of the lognormal distribution were set equal, respectively, to the lower and upper limits.

At each point in the RWMS the sample mean, 2.5th percentile, and 97.5th percentile were calculated from the realizations. These are displayed in Figures 6, 7, and 8, respectively. Figure 6, in which the sample mean is displayed, is similar to Figure 5, in which no uncertainty is accounted for. Hence, despite model nonlinearity which might have lead to complex error propagation, uncertainties of the magnitudes considered here have little impact on mean estimated elevation. Figures 7 and 8 display percentiles of the sampling distribution. Unlike the piezometric head itself, there is no reason these surfaces should obey Equation 1.

The roughness of Figures 7 and 8 can be attributed to surface "flatness." That is, the curvature of the surface is so small that, comparatively, Monte Carlo sampling error is nonnegligible. This would not hold if the surface curved more sharply, as demonstrated by Monte Carlo studies (not reported here) using elevations resulting in less flat surfaces. Standard deviation of sampling error is inversely proportional to the square root of the number of realizations. Hence, the number of realizations required for negligible sampling error is impractically large.

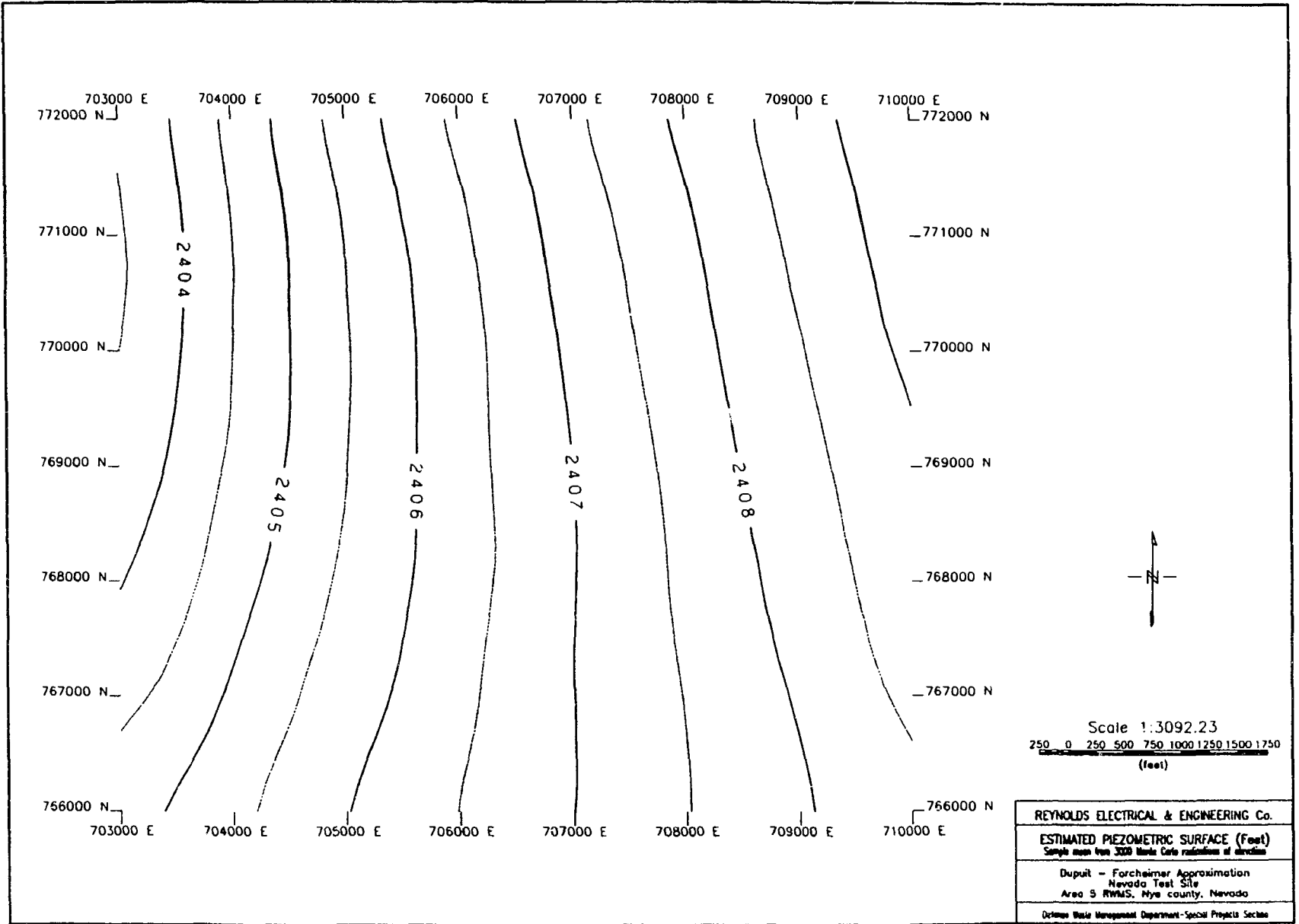


Figure 6. Sample mean from 3,000 Monte Carlo realizations of water table elevation.

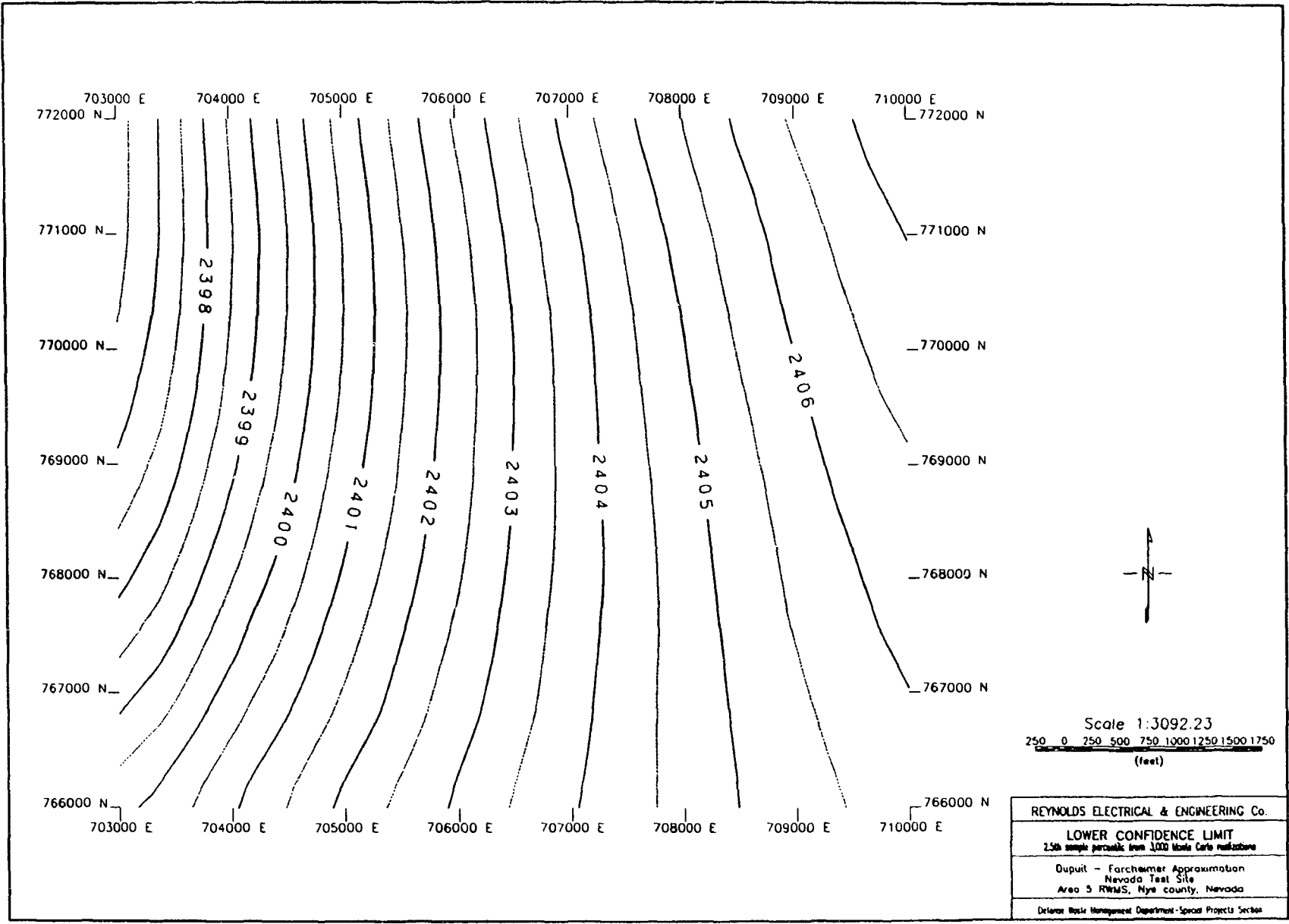


Figure 7. 2.5th sample percentile from 3,000 Monte Carlo realizations of water table elevation.

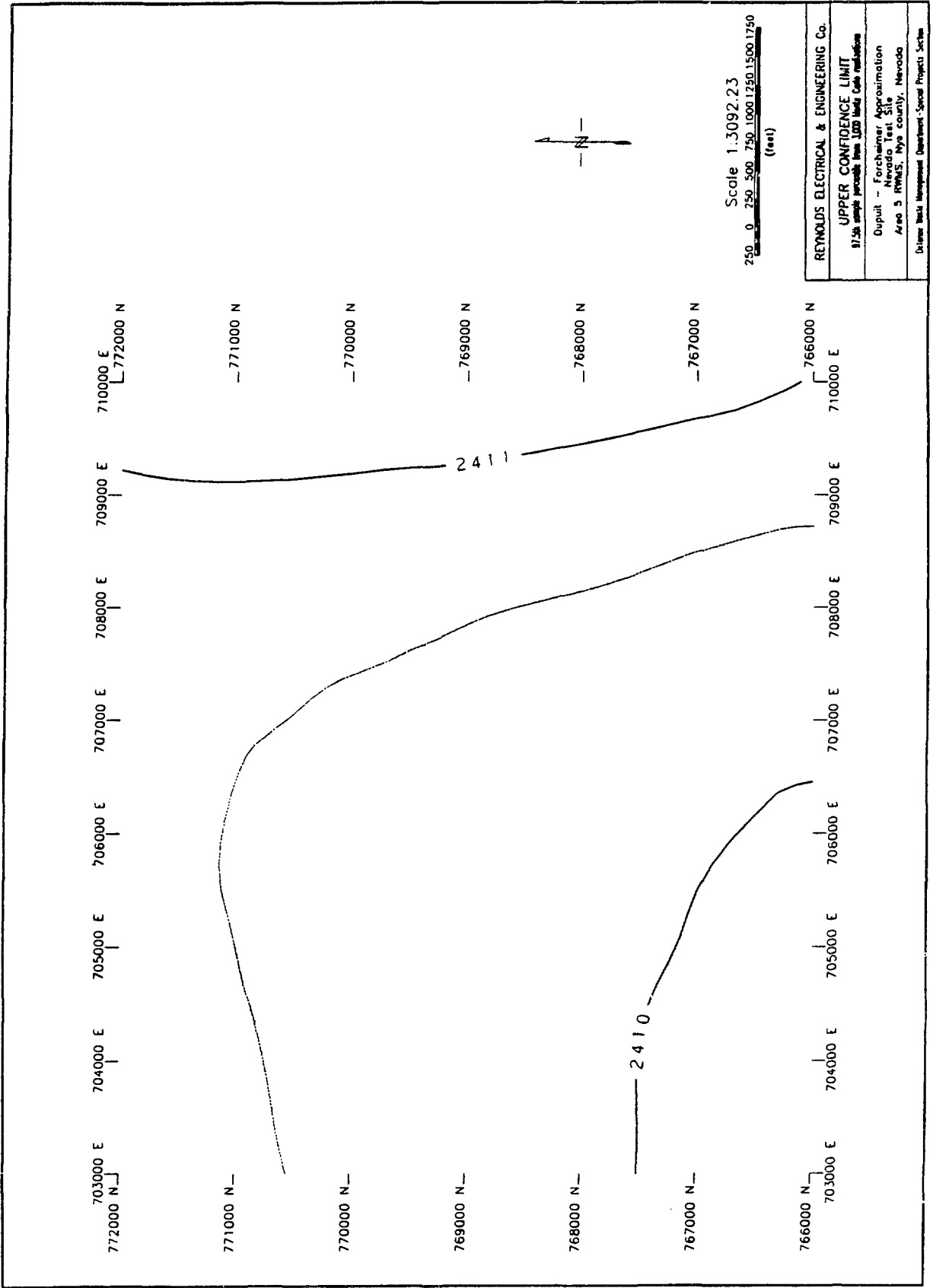


Figure 8. 97.5th sample percentile from 3,000 Monte Carlo realizations of water table elevation.

Figures 7 and 8, taken together, provide point-by-point approximate 95 percent confidence intervals for estimated elevation. These are flat enough to render identification of gradient direction impossible. However, they do show the magnitude of the gradient is small. Hence, any flow would be slow, though of unknown direction. Figure 8 somewhat counterintuitively has a local minimum. To understand why, let $E(x,y)$ denote the estimated elevation at a point (x,y) and let $S(x,y)$ be its estimated standard deviation. Treating estimates as normally distributed, though not strictly mathematically correct, facilitates exposition.

Under this assumption, an approximate 95 percent confidence interval for $E(x,y)$, the true mean is $E(x,y) \pm 2 S(x,y)$. In general, $E(x,y)$ increases in X (water table elevations are greater to the east) but $S(x,y)$ decreases in X (uncertainty concerning water table elevations is greater to the west, where there are fewer nearby wells/drill holes). Hence, the upper confidence limit [$E(x,y) + 2 S(x,y)$] is the sum of an increasing and decreasing function. It is not surprising such a sum has a local minimum. The lower confidence limit [$E(x,y) - 2 S(x,y)$] is the sum of two functions increasing in X and exhibits no local extrema.

5.0 INFILTRATION/EVAPORATION

5.1 Infiltration (direct surface recharge)

So far q_{rchg} has been set to zero in all simulations. The reason for this is that we have been unable to find any published work on direct recharge estimation conducted near the RWMS in Area 5 of the NTS. Chloride mass balance methods for estimating q_{rchg} do exist and have been used by Stone (1985) in estimating the effect of various surface coverings over calcareous alluvium in New Mexico and Western Australia. They have also been used by Scanlon (1991) in estimating recharge in western Texas desert soils. However, the assumptions on which the chloride mass balance and isotopic chlorine methods rest may not be valid for the extremely dry high desert conditions of Frenchman Flat, Nevada (Scanlon, 1991).

In the interest of seeing the effects of a nonzero direct recharge, two additional water table simulations have been made. In the first case q_{rchg} was set at 0.003 ft/day. This is equivalent to slightly over one foot of water per year. Figure 9 shows the result of setting q_{rchg} to +0.003 ft/day and estimating the water table using the calibration data listed in Table 2.

5.2 Evaporation (direct surface exfiltration)

In the second case q_{rchg} was set at -0.003 ft/day which, again, is equivalent to slightly over one foot of water evaporated per year. Figure 10 shows this simulation. In this case the current calibration well data (Table 2) were used.

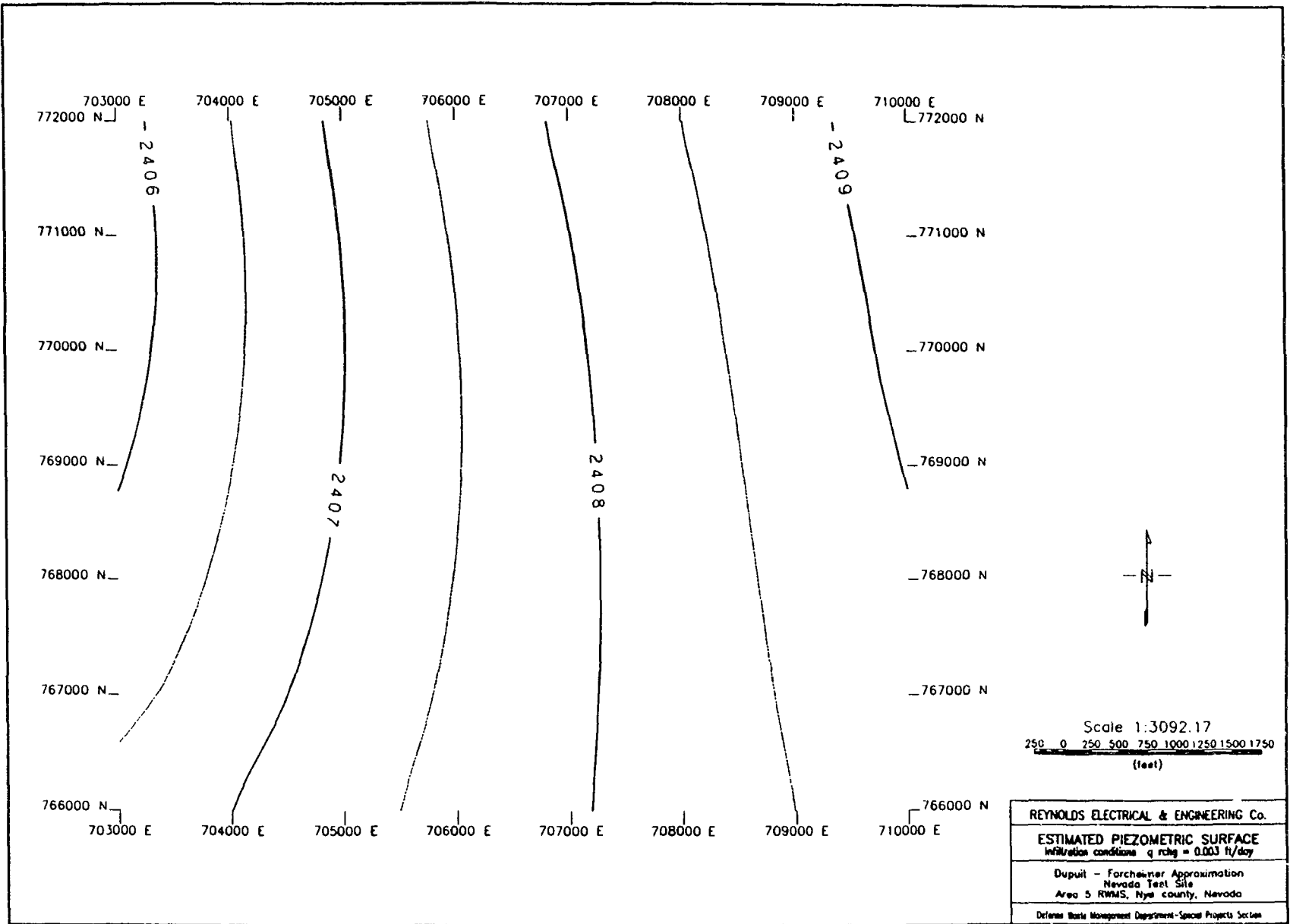


Figure 9. Estimated water table under RWMS when $q_{rchg} = 0.003$ ft/day (infiltration conditions).

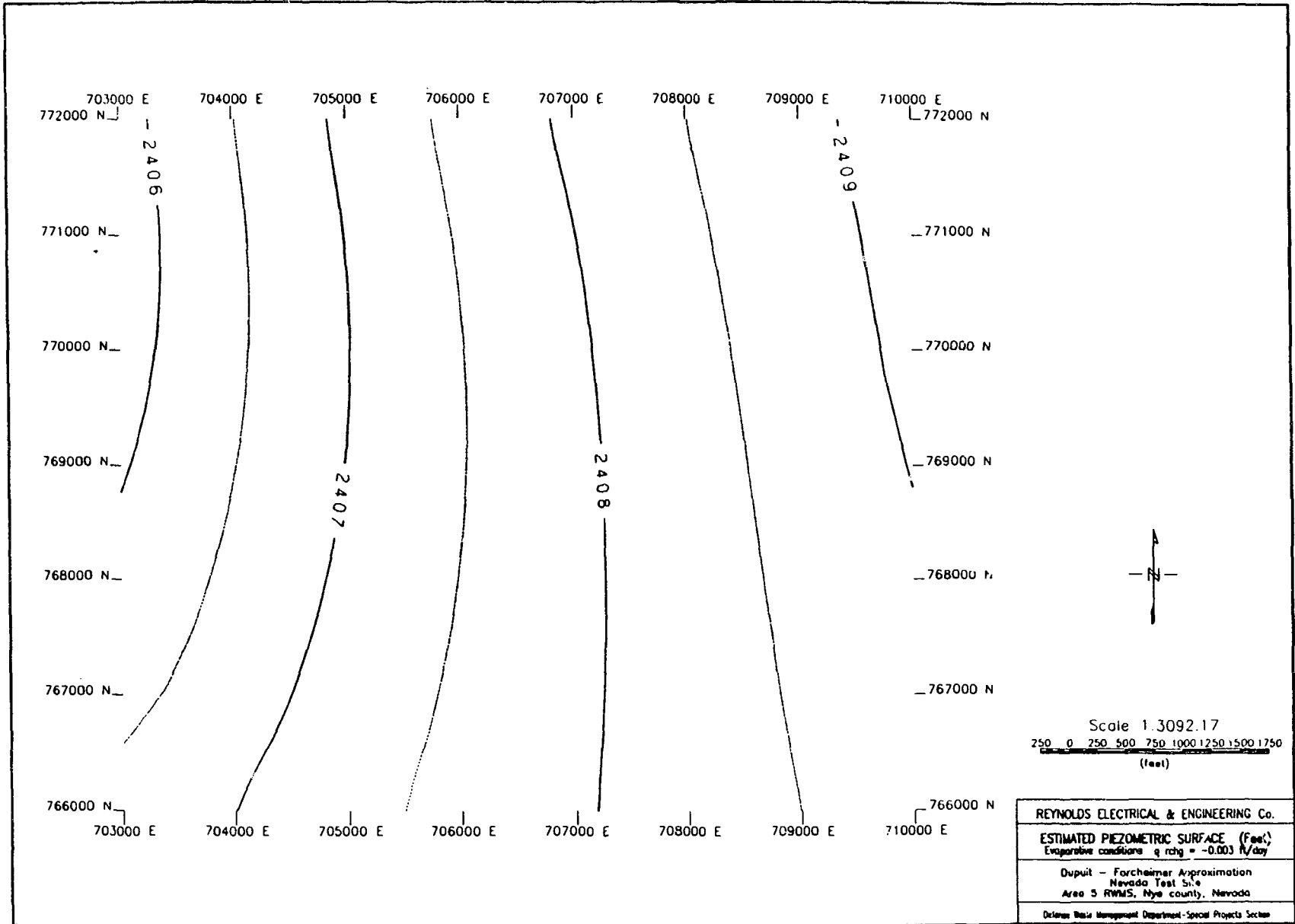


Figure 10. Estimated water table under RWMS when $q_{rchg} = -0.003$ ft/day (evaporative conditions).

Comparison of Figure 5, where the estimated water table has been computed using $q_{rchg} = 0$, with Figure 9 ($q_{rchg} = +0.003$ ft/day) and Figure 10 ($q_{rchg} = -0.003$ ft/day) clearly shows that infiltration causes a slight elevation increase, whereas evaporation causes a slight elevation decrease in the water table surface. Since q_{rchg} is realistic but small, the effect is to produce a small perturbation; hence Figures 9 and 10 are very similar. Since the scale used here is of the order of 25,000 feet and since the RWMS is off to the northwestern side of the region of model calibration, these figures show that very little effect on the water table elevations is expected under either direct recharge or direct evaporation. Indeed, using $q_{rchg} = 0.003$ ft/day, obtained from the Winograd and Thordarson (1985) precipitation map, is probably three to four orders of magnitude too high. Much smaller values, either positive or negative, of q_{rchg} will have a much smaller effect on an already small effect. Thus, it is our opinion that direct recharge and/or evaporation may be neglected in any further use of the two-dimensional water table estimator model DUP3D8P (Lindstrom et al. 1992).

6.0 CONCLUSIONS AND FUTURE WORK

The feasibility of using the Dupuit-Forcheimer modeling assumptions for estimation of the water table under the RWMS in Area 5 of the NTS has been clearly established in this work. However, it remains to be seen via direct validation boreholes around the RWMS border that the models predictions are accurate. The belief in the hypothesis that the water table under the RWMS is "flatter than a pancake" is still strong (Cox, 1991). Unfortunately the state of the art in deep borehole drilling is such that the U.S. Department of Energy rightfully refuses to allow any surface-to-water table drilling within the boundaries of the RWMS itself. The potential for creating direct leaks or direct transport paths from the surface to the water table if a "swiss cheese" type drilling operation were to be allowed is too great. Therefore, it is doubtful that a direct validation of the accuracy of the D-F model discussed here in for the RWMS will be achieved. The D-F model discussed herein can, however, be validated using surface-to-water table borehole data around the boundaries of the RWMS. The three initial RWMS boundary characterization surface-to-water table boreholes are currently being drilled. These three water table elevations will be used as a direct check on the "degree of goodness" of the estimated water table under the RWMS.

As was stated earlier in the warning about the potentially singular nature of design matrix X if a "bad" geometric well pattern is chosen, work is currently under way to discover the properties of X if the well pattern is perturbed away from these designs.

Efforts are currently under way to conduct a joint well pattern design research project with Desert Research Institute staff hydrologists with an eye toward using the D-F model to aid in choosing an "optimal" design. For example, the classical designs based upon D-optimality (determinant) yielding minimum covariance matrix components, or K-optimality (spectral condition number) yielding well-conditionedness of the design matrix or some weighted combination of both D and K optimality criteria will be considered. Simple extension of the D-F model from using eight calibration

well data sets (the purely interpolatory case) to nine or more calibration well data sets and a variational (least squares) concept also gives rise to the same type of optimality criterion.

In all the above cases the D-F model DUP3D8P is used essentially in the "inverse mode." That is, we are solving an inverse or parameter estimation problem. Another inverse mode use of the D-F model is that of locating hidden geologic structures. For example, suppose that \underline{A} and \underline{B} have been determined from eight calibration well logs and that q_{rchg} has been defined at the four outer calibration points. Then, if an absurdly large mound or depression in the water table is predicted, it probably indicates the assumptions of the models are being violated. This in turn means hidden geologic or hydrologic structures (e.g., faults, fractures, springs, drains) are present. Virtually no use of the D-F model has been made to date with respect to this last concept. However, as more data become available we plan to use the model to "prospect" for hidden structures.

7.0 LITERATURE CITED

Bear, J. and A. Verruijt (1987)

Modeling ground water flow and pollution: theory and applications of transport in porous media. Reidel, Dordrecht, 414 pp.

Box, G.E.P., W. G. Hunter, and J. S. Hunter (1978)

Statistics for Experimenters: An introduction to design, data analysis, and model building. Wiley, New York, 653 pp.

Carslaw, H. S. and J. C. Jaeger (1957)

Conduction of heat in solids. Oxford Press, 510 pp.

Case, C. J. Davis, R. French, and S. Raker (1984)

Site characterization in connection with the low level Radioactive Waste Management Site in Area 5 of the Nevada Test Site, Nye County, Nevada - Final Report, USDOE/NV/10163-13. Reynolds Electrical & Engineering Co., Inc., P.O. Box 98521, Las Vegas, NV 89193-8521.

Cox, Warren (1991)

Private communication

Daffern, D. D., L. L. Ebeling, and W. B. Cox (1990)

Unsaturated zone characterization of the Area 5 Radioactive Waste Management Site: Phase I. Preliminary laboratory studies for the determination of soil moisture characteristic curves and unsaturated hydraulic conductivities. U.S. Department of Energy Report, USDOE/NV/10630-3. Reynolds Electrical & Engineering Co., Inc., P.O. Box 98521, Las Vegas, NV 89193-8521.

Dozier, B. L., and S. E. Rawlinson (1991)

Conceptual model for the geology in Area 5. U.S. Department of Energy Report, USDOE/NV/10630-14. Reynolds Electrical & Engineering Co., Inc., P.O. Box 98521, Las Vegas, NV 89193-8521.

Dupuit, J. (1863)

Etudes theoriques et pratiques sur le mouvement des eaux dans les canaux decouverts et à travers les terrains perm éables. Dunod, Paris.

Hantush, M.S. (1967)

Growth and decay of groundwater mounds in response to uniform percolation. Water Res. Res 3:227-234.

Lindstrom, F. T., L. E. Barker, D. E. Cawfield, D. D. Daffern, B. L. Dozier, D. F. Emer, and W. R. Strong (1992)

Estimating the water table under the Radioactive Waste Management Site in Area 5 of the Nevada Test Site: the Dupuit-Forcheimer approximation. U.S. Department of Energy Report, USDOE/NV/10630-24. Reynolds Electrical & Engineering Co., Inc., P.O. Box 98521, Las Vegas, NV 89193-8521.

Neagle, C. C. (1992)

Personal communication.

Prenter, P. M. (1975)

Splines and variational methods. Wiley, New York, 323 pp.

Winograd, I. J. and W. Thordarson (1975)

Hydrogeologic and hydrochemical framework, South-Central Great Basin, Nevada-California, with special reference to the Nevada Test Site: hydrology of nuclear test sites. USGS prof. paper #712-C, U.S. Govt. Printing Office, Washington, DC.

Young, D. M., and R. T. Gregory (1973)

A Survey of Numerical Mathematics: Volume II. Addison-Wesley, Reading, MA.

8.0 NOMENCLATURE

I.	Dependent Variables		
	<u>Symbols</u>	<u>Meaning</u>	<u>Units</u>
	$H(x,y)$	Water table elevation above mean as the datum	(ft)
	$H_L(x,y)$	Laplace water table elevation	(ft)
	$H_p(x,y)$	Poisson water table elevation	(ft)
II.	Independent Variables		
	<u>Symbols</u>	<u>Meaning</u>	<u>Units</u>
	x	Easting Nevada Coordinate	(ft)
	y	Northing Nevada Coordinate	(ft)
III.	Liquid Fluxes		
	<u>Symbols</u>	<u>Meaning</u>	<u>Units</u>
	q_x	Easting Darcy flux if positive and westing flux if negative	(ft/day)
	q_y	Northing Darcy flux if positive and southing flux if negative	(ft/day)
IV.	Fluid and Porous Medium Properties		
	<u>Symbols</u>	<u>Meaning</u>	<u>Units</u>
	K	Saturated hydraulic conductivity (20°C)	(ft/day)
V.	Infiltration of Evaporation Rate		
	<u>Symbols</u>	<u>Meaning</u>	<u>Units</u>
	q_{rchg}	Infiltration (+) or evaporation (-) rate reflective of vertical hydraulic conductivity property of porous medium	(ft ³ /ft ² -day)

9.0 APPENDIX A

The eight basic functions, all of which satisfy the Laplace partial differential equation, $\frac{\partial^2 \Phi}{\partial x^2} + \frac{\partial^2 \Phi}{\partial y^2} = 0$, and used in the D-F model DUP3D8P, are defined as:

$$\Phi_0(x,y) = 1.0 \quad (\text{A.1})$$

$$\Phi_1(x,y) = x - x_0 \quad (\text{A.2})$$

$$\Phi_2(x,y) = (x - x_0)^2 - (y - y_0)^2 \quad (\text{A.3})$$

$$\Phi_3(x,y) = (x - x_0) \left((x - x_0)^2 - 3(y - y_0)^2 \right) \quad (\text{A.4})$$

$$\Phi_4(x,y) = y - y_0 \quad (\text{A.5})$$

$$\Phi_5(x,y) = (x - x_0)(y - y_0) \quad (\text{A.6})$$

$$\Phi_6(x,y) = (y - y_0) \left((x - x_0)^2 - \frac{1}{3}(y - y_0)^2 \right) \quad (\text{A.7})$$

$$\Phi_7(x,y) = (x - x_0)(y - y_0) \left((x - x_0)^2 - (y - y_0)^2 \right) \quad (\text{A.8})$$